Current Topics in Peptide & Protein Research
Vol. 16, 2015

Original Communication

Modulating the dysregulated migration of pulmonary arterial hypertensive smooth muscle cells with motif mimicking cell permeable peptides

Jamie L. Wilson[1,*], Chamila Rupasinghe[2], Anny Usheva[3], Rod Warburton[4], Chloe Kaplan[1], Linda Taylor[1], Nicholas Hill[4], Dale F. Mierke[2] and Peter Polgar[4]

[1]Department of Biochemistry, Boston University School of Medicine, Boston, Massachusetts; [2]Department of Chemistry, Dartmouth College, Hanover, New Hampshire 03755; [3]Department of Surgery, Warren Alpert Medical School, Brown University, Providence, Rhode Island 02903; [4]Tupper Research Institute and Pulmonary, Critical Care, and Sleep Division, Tufts Medical Center, Boston, Massachusetts 02111, USA.

ABSTRACT

Migration of vascular smooth muscle cells is a key element in remodeling during pulmonary arterial hypertension (PAH). We are observing key alterations in the migratory characteristics of human pulmonary artery smooth muscle cells (HPASMC) isolated from transplanted lungs of subjects with PAH. Using wound migration and barrier removal assays, we demonstrate that the PAH cells migrate under quiescent growth conditions and in the absence of pro-migratory factors such as platelet derived growth factor (PDGF). Under the same conditions, in the absence of PDGF, non-PAH HPASMC show negligible migration. The dysregulated migration initiates, in part, through phosphorylation events signaled through the unstimulated PDGF receptor via focal adhesion kinase (FAK) whose total basal expression and phosphorylation at tyrosine 391 is markedly increased in the PAH cells and is inhibited by a motif mimicking cell-permeable peptide (MMCPP) targeting the Tyr751 region of the PDGF receptor and by imatinib. However, exposure of the PAH cells to PDGF further promotes migration. Inhibition of p21 activated kinases (PAK), LIM kinases (LIMK), c-Jun N-terminal kinases (JNK) and p38 mitogen-activated protein kinases (MAPK) reduces both the dysregulated and the PDGF-stimulated migration. Immunofluorescence microscopy confirms these observations showing activated JNK and p38 MAPK at the edge of the wound but not in the rest of the culture in the PAH cells. The upstream inhibitors FAK (PF-573228) and imatinib block this activation of JNK and p38 at the edge of the site of injury and correspondingly inhibit migration. MMCPP which inhibit the activation of downstream effectors of migration, cofilin and caldesmon, also limit the dysregulated migration. These results highlight key pathways which point to potential targets for future therapies of pulmonary hypertension with MMCPP.

KEYWORDS: pulmonary arterial hypertension, vascular smooth muscle cells, cell migration, p38 MAPK, c-Jun N-terminal kinases (JNK), platelet-derived growth factor (PDGF)

ABBREVIATIONS

HPASMC, Human pulmonary artery smooth muscle cells; PAH, pulmonary arterial hypertension; MMCPP, motif mimicking cell-permeable peptides; CaD, caldesmon.

*Corresponding author: jlwilson@bu.edu

INTRODUCTION

Vascular smooth muscle cell migration participates in the pathology of many vascular diseases including pulmonary arterial hypertension (PAH), restenosis and atherosclerosis [1, 2]. In PAH, migration in conjunction with proliferation of smooth muscle and endothelial cells is a major contributor to vascular remodeling of distal pulmonary arteries leading to hypertrophy of vascular media and intima [3, 4], severe vascular resistance [5], increased pulmonary arterial pressure and formation of plexiform lesions [6]. Although no such evidence has yet been reported with human pulmonary artery smooth muscle cells (HPASMC), a recent report by Sheikh *et al.* (2014) [7] traced smooth muscle cells in distal pulmonary arterioles in hypoxic mice and found that these pathological smooth muscle cells originate from pre-existing smooth muscle cells. This further suggests that the smooth muscle cells originating in the vessel media are migrating into the vessel lumina and then proliferating. Thus, limiting or abrogating smooth muscle cells from migrating could be a strong contributing strategy for the treatment of PAH. At this time, this process in its entirety is poorly understood and needs further mechanistic investigation.

Previous studies have shown that PAH induces proliferation and decreases apoptosis of pulmonary artery smooth muscle cells [8-10]. Additionally, the pathological alterations of these cells also increase their pro-migratory potentials. The platelet-derived growth factor (PDGF) receptors which are known to participate in the proliferation and migration of smooth muscle cells (SMC), have increased levels of expression in pulmonary arteries from idiopathic PAH (IPAH) patients [11]. In the same study, imatinib was shown to inhibit PDGF-stimulated migration of SMC [11]. Imatinib is a tyrosine kinase inhibitor known to regulate Abelson murine leukemia viral oncogene homolog 1 (ABL1) and the PDGF receptors [12]. Similarly, focal adhesion kinase (FAK) has been well established to be involved in cell motility in various cell types [13, 14].

Herein we identify downstream targets related to cytoskeletal dynamics which reduce the migration of HPASMC isolated from patients with PAH. These targets include PAK and LIMK and actin binding regulators cofilin and caldesmon (CaD) [15-19]. Our approach involves inhibiting the activation of these targets with motif mimicking cell permeable peptides (MMCPP). We previously demonstrated that PDGF-promoted migration in HPASMC can be limited with a MMCPP targeting the PDGFβ receptor (PDGFR) [20]. Here, we illustrate that PAH migration involves PDGFR and FAK cascades which encompass p38 and JNK. Also, MMCPP aimed at downstream targets of cell migration such as CaD and cofilin are used to modulate the PAH HPASMC migration. Thus, we observe that HPASMC from PAH patients undergo a dysregulated, markedly enhanced migration in the absence of effector stimulation. The signal for this dysregulated migration is in part promoted through an unstimulated PDGFR and then channeled through an already activated FAK which then signals downstream through PAK/LIMK/JNK leading to the phosphorylation of cofilin and CaD. These observations on PAH-related HPASMC migration have not been reported previously and should form a new and very important explanation of the remodeling process taking place in PAH.

MATERIALS AND METHODS

Chemicals

ML 141, PF-573228 and aphidicolin were purchased from Sigma-Aldrich (St. Louis, MO) and LIMKi3 from Calbiochem EMD Millipore (Billerica, MA), and Y27632, SB203580, SP600125 and NSC23766 were purchased from Cayman Chemical (Ann Arbor, Michigan). IPA3 was purchased from Tocris Biosciences (Minneapolis, MN) and PDGF-BB (PDGF) from R&D Systems (Minneapolis, MN).

Peptide synthesis

The different MMCPPs are composed of the targeting sequence and the cell penetrating sequence (SynB3:RRLSYSRRRF) [21]. All the compounds were synthesized by Fmoc-based solid-phase peptide synthesis protocols employing microwave heating (CEM Discover S-class microwave synthesizer), using the appropriately protected amino acids. All compounds were synthesized on Rink-Amide-ChemMatrix resin (Nmmol, 0.6 mmol/g,

P/N no. 7-600-1310-25), using HBTU (2-(1H-benzotriazol-1-yl)-1,1,3,3-tetramethyluronium hexafluorophosphate) for coupling and piperidine for Fmoc deprotection as detailed elsewhere [22]. The compounds were then purified by reversed phase high performance liquid chromatography, and molecular mass confirmed by matrix-assisted laser desorption ionization-time of flight mass spectroscopy.

Cell culture

Human pulmonary artery smooth muscle cells were a generous gift of Drs. Erzurum and Comhair of the Cleveland Clinic (Cleveland, OH). The cells used in this study were obtained from non-PAH (n = 3), IPAH (n = 4) and hereditary PAH (HPAH) (n = 2) donor subjects [23]. Subjects were identified as having PAH based on the National Institutes of Health (NIH) registry diagnostic criteria for pulmonary hypertension. Non-PAH individuals had no history of pulmonary or cardiac disease or symptoms. A description of these individuals is given in table 1. Cells were isolated from elastic pulmonary arteries (>500 µm diameter) after dissection from lungs obtained at explantation during lung transplant as described by Comhair *et al.*, 2012 [24]. Cells were cultured in complete medium containing 15 mM HEPES (4-(2-hydroxyethyl)-1-piperazineethanesulfonic acid) buffered Dulbecco's Modified Eagle Medium (DMEM)/F12 (50:50) media (Mediatech, Manassas, VA) containing 10% fetal bovine serum (FBS) (Lonza), and 2.5% Antibiotic-Antimycotic from GIBCO (cat. no. 15240). Quiescence medium contained the same ingredients as complete medium except that the FBS concentration was reduced to 0.2%. Primary cultures of passages 6-10 were used in experiments.

Wound migration assay

HPASMC were grown to confluence on 12-well culture plates in complete medium. Once confluent, the medium was changed to 0.2% FBS medium (quiescence medium) overnight. The next day, a wound was induced by scrapping off a portion of the cell monolayer down the middle of the well with a P1000 tip. Perpendicular to the wound a straight line was drawn with a marker to better identify the same wound location under a microscope. After the wound was made, the medium in each well was replenished with new quiescence medium. When applicable, additives such as anti-PDGF neutralizing antibody #06127 from EMD Millipore (Billerica, MA), mouse IgG control sc-2025 from Santa Cruz Biotechnology (Santa Cruz, CA), or other additives listed under chemicals were added and images were taken of each wound in fields above and below the drawn line at time 0. In experiments where the cells were growth arrested, 10 µM aphidicolin was added to the quiescence medium, wound inflicted and then the medium was replenished either with or without 10 µM of aphidicolin. The cultures were then incubated at 37 ^{o}C, 5% CO_2 for 24 hours.

Table 1. Information on human pulmonary artery smooth muscle cells.

Subject	Gender	Age	Germline mutation
Donor controls	-	-	-
Non-PAH1	Male	36	None
Non-PAH2	Male	39	None
Non-PAH3	Female	48	None
PAH subjects	-	-	-
HPAH1	Male	41	Deletion Exon 1-8
HPAH2	Female	50	Deletion Exon 4-5
IPAH1	Female	34	None
IPAH2	Female	39	None
IPAH3	Male	52	None
IPAH4	Male	42	None

After incubation, cells were stained with 20% methanol/PBS (Phosphate-buffered saline) crystal violet solution. Each wound area was imaged in the same fields as before at 40X magnification. Migrations were determined by counting the number of cells which migrated into the wound, excluding the cells on the edges. This analysis was quantified by using ImageJ software [25]. The average and the standard deviation of each treatment were taken from triplicate wells and the experiments were done with at least three biological replicates.

Migration following barrier removal

Ibidi culture-inserts are composed of a biocompatible silicon material that sticks to the bottom of the well and contains two reservoirs separated by a 500 µm wide barrier. The Ibidi culture-inserts were each placed inside the wells of a 12-well cell culture plate. Once culture-inserts were secure at the bottom of each well, a cell suspension of HPASMC was added to each reservoir in a total volume of 70 µL and incubated at 37 ^{o}C, 5% CO_2 overnight. The next day quiescence medium was added and the cells were incubated for 24 hours. Next, the culture-inserts were removed and 1 mL of fresh quiescence medium was added with or without additives. A line perpendicular to and at the midpoint of the barrier was drawn under the plate. Immediately, time 0 images were taken at 40X magnification of fields above and below the marked line and the cultures were incubated for another 24 hours at 37 ^{o}C, 5% CO_2 before final images were taken.

Immunofluorescence of wound border area

HPASMC were seeded to confluence on round coverslips inside the 12-well plates in complete medium. Once confluent, the medium was changed to quiescence medium and the cells were incubated for 24 h. In some experiments, cells were pretreated for 1 h with the respective inhibitors. After incubation, wounds were made to the coverslips by scrapping off a portion of the cell monolayer down the middle of the well with a P1000 tip and they were re-incubated for 15 min. Next, the plates with the coverslips were placed on ice and cells were fixed with 4% paraformaldehyde, washed 3 times with cold PBS and then permeabilized with 0.5% Triton X-100 in PBS. After additional washes with PBS, coverslips were then blocked using casein blocking buffer and were incubated overnight at 4 °C with one of the following primary antibodies diluted in blocking buffer solution: phospho-JNK (p-JNK) (Promega #V793A) at (1:50), phospho-ERK (p-ERK) (Cell Signaling #9101) at (1:80) or phospho-p38MAPK (p-p38) (Cell Signaling #4511) at (1:400). On the next day the coverslips were washed 3 times with wash buffer (0.05% Tween 20, 0.02% saponin in PBS), and then incubated with Alexa 488-conjugated anti-rabbit secondary antibody (Life Technologies #A-21441) at 1:300 for 1 h, washed a final time and mounted on slides using ProLong® gold antifade mountant with DAPI (4',6-diamidino-2-phenylindole) (Life Technologies). Fluorescence microscopy (Nikon Eclipse TE200 fluorescence microscope) was used to detect FITC (fluorescein isothiocyanate) and DAPI staining on the wound edges. Images were taken at 200X magnification using Spot software (Diagnostic Instruments). Adjustment of image brightness and contrast were performed with ImageJ and Adobe Photoshop. Quantitation of fluorescence was performed using ImageJ as done by Burgess *et al.*, 2010 [26]. In brief, each cell on the edge of the wound was individually measured for integrated density and area. Then, corrected total cell fluorescence (CTCF) was calculated by taking integrated density minus (selected area) multiplied by the mean fluorescence of background readings. CTCFs were averaged across all cells on the edge.

Western blot

Cells were seeded in 6-well cell culture plates until confluence was reached. At that point, their medium was replaced with quiescence medium and the cultures were incubated overnight. Then, they were treated with or without either 10 uM PF-573228 or 5 uM imatinib for 1 h. Afterwards, cells were lysed using 100 µl Radio-Immuno-precipitation Assay (RIPA) buffer (150 mM NaCl, 1.0% Igepal CA-630, 0.5% sodium deoxycholate, 0.1% sodium dodecyl sulfate (SDS), and 50mM Tris, pH 8.0 (Sigma, St Louis, MO)) containing both complete protease inhibitor cocktail and PhosSTOP phosphatase inhibitor cocktail (Roche Applied Science, Indianapolis, IN) and total

protein was isolated from each well. Total protein was quantified using bicinchoninic acid assay (BCA). Equal amounts of protein were loaded and electrophoresed on SDS-polyacrylamide gel electrophoresis (PAGE) with a 4% stacking and 7% separating gel. Proteins were then transferred to an Invitrolon Polyvinylidene fluoride (PVDF) membrane (Life Technologies, Carlsbad, CA) at 100 V and 4 °C for 2 hours. The PVDF membranes were blocked at room temperature for 1 hour with 5% powdered milk in Tris-buffered saline with Tween 20 (TBS-T) (20 mM Tris, 150 mM NaCl, and 0.1% Tween 20, pH 7.6). Then, membranes were incubated overnight with primary rabbit antibody pFAK(Tyr397) (#8556) or total FAK (#13009) (Cell Signaling, Danvers, MA) at 4 °C in a solution TBS-T with 5% Bovine serum albumin (BSA) at 1:1000 dilution. Blots were washed again in TBS-T followed by 1 h incubation in the corresponding anti-rabbit secondary antibody (Cell Signaling, Danvers, MA) in a solution of TBS-T at 1:2000 dilution. Blots were then washed in TBS-T, and developed in detection reagents from Thermo Scientific (Rockford, IL) for 1 min before exposure to autoradiography film. Densitometry on band intensities was performed using the NIH ImageJ image analysis software [25].

Cell viability

The effects of pharmacological inhibitors and MMCPP on cell viability were evaluated using the MTT assay. The assay is based on the detection of the reduction of yellow MTT (3-(4, 5-dimethyl-thiazolyl-2)-2, 5-diphenyltetrazolium bromide) by metabolically active cells to purple formazan which is then quantified spectrophotometrically at 570 nm. HPASMC were seeded in 96-well plates and cultured to 90% confluence. Medium was changed to quiescence medium and cells were incubated with pharmacological inhibitors or MMCPP for 24 h before the MTT assay was performed. Cell viability was measured as the optical density (OD) value at 570 nm using a biotek synergy multi-mode microplate reader (Biotek, Winooski, VT, USA). All treatments were performed in at least triplicate wells.

Statistics

As appropriate, data were presented as means with standard deviations and were evaluated for statistical significance by a one-way analysis of variance (ANOVA) and Tukey's post hoc test with p values < 0.05 considered significant.

RESULTS

Cell migration in non-PAH and PAH HPASMC

In a previous communication we demonstrated that both PAH and non-PAH HPASMC retain their phenotype in culture [9]. HPASMC derived from PAH and non-PAH subjects were tested for their migratory response. Using the culture wound model the cell monolayers were monitored for cell movement into the wound area. In the absence of any pro-migratory factors, the number of cells that migrated into the wound area was markedly elevated in PAH HPASMC compared to non-PAH controls. As illustrated in fig. 1A, both the HPAH and IPAH derived HPASMC displayed similar highly active migration into the wound area while non-PAH migration was negligible**.** Fig. 1B shows that migration by four IPAH and two HPAH strains into the wound is significantly elevated relative to three non-PAH cell strains. Some variation among the PAH strains was observed but all were significantly higher compared to the non-PAH cell migration. Typically, the non-PAH strains showed very little non-stimulated migration.

The markedly increased number of PAH HPASMC in the wound area compared to the non-PAH cell number could not be attributed to greater proliferation of the PAH cells, since the doubling time for the HPASMC cells is approximately 94 h [9]. Furthermore, the wound migration assay was also performed with the inclusion of the cell cycle arresting agent aphidicolin in the medium and analogous migration results were obtained (Fig. 1C).

To confirm the dysregulated migration of PAH cells, we used an alternative assay, the barrier removal procedure, which does not involve wounding. In this assay, cells were cultured in wells containing an insert 500 μm wide which separated two confluent HPASMC populations. Twenty-four hours after barrier removal, the number of cells which migrated into the barrier space was determined. The results were comparable to those from the wound assay (Fig. 1D). Subsequent migration experiments were performed with the wound assay.

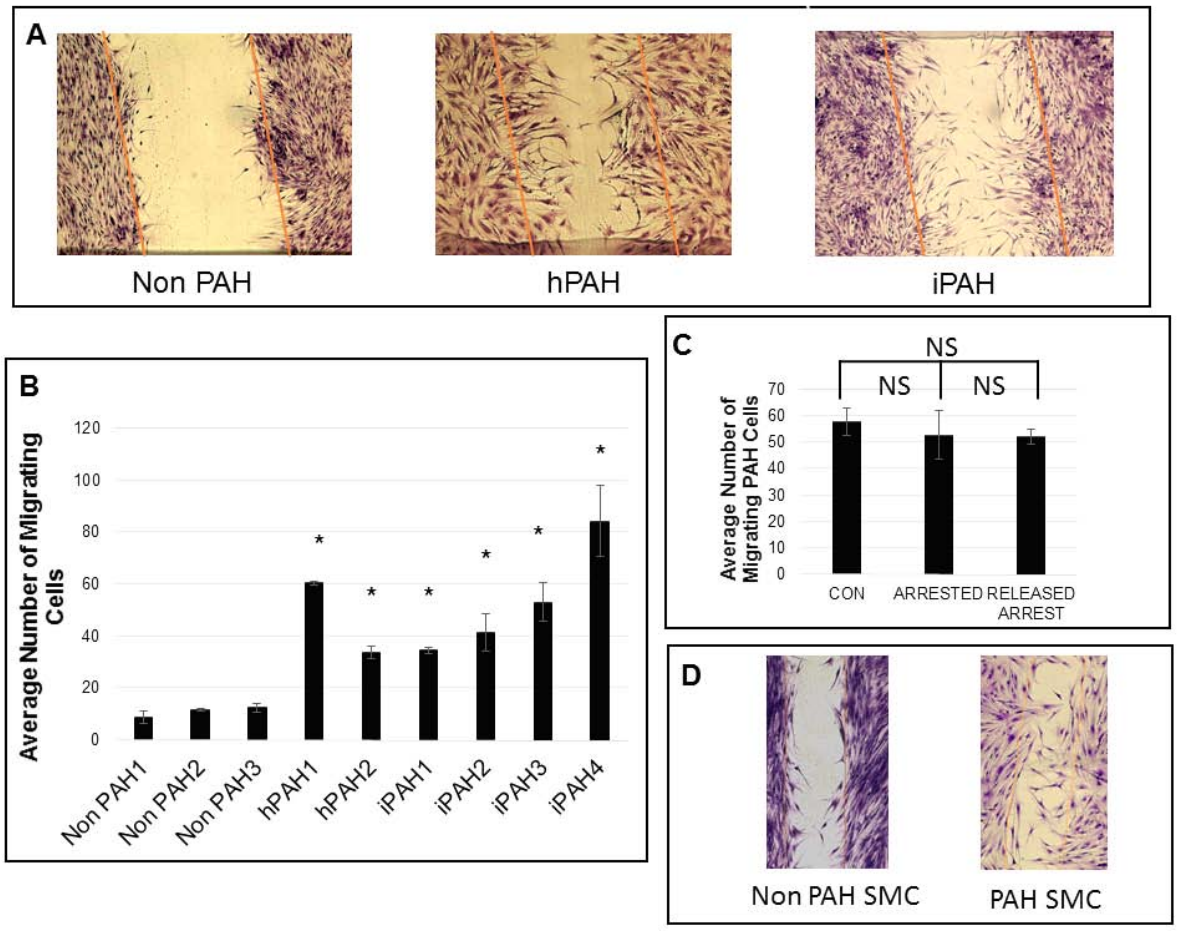

Fig. 1. Average migration of PAH vs non-PAH HPASMC. (A) A wound assay was performed on confluent HPASMC in quiescence medium and the number of cells that migrated into the wound after 24 hours was measured in various HPASMC. A representative image showing migration of non-PAH, HPAH and IPAH HPASMC is shown. The orange lines represent the cell borders at time 0 of the wound. (B) Bar graphs represent the average number of cells from different cell strains (n = 3 non-PAH, n = 2 HPAH or n = 4 IPAH HPASMC) that migrated into the wound in at least triplicate wells. The standard deviation is represented by the error bars. These results are representative of at least triplicate experiments. *$p < 0.05$ vs non-PAH. (C) Migration of PAH HPASMC during growth arrest. PAH HPASMC were measured for wound migration with (arrested) and without (CON) the presence of cell cycle inhibitor aphidicolin (10 uM). After wounding, medium with or without arresting agent (released arrest) were added and the number of cells migrating into the wound were determined. NS, nonsignificant. (D) Barrier removal migration of HPASMC. Non-PAH and PAH HPASMC were seeded in reservoirs separated by a barrier 500 uM apart. After the cells attach to the bottom of the plate (overnight), the culture medium was changed to quiescence medium and the cells were incubated for 24 h. The barrier was then removed allowing for migration of cells into the open region between reservoirs. Image shows migration of cells into the open region 24 h after barrier removal. The orange lines denote the original edges of the cell reservoirs.

Agonist stimulated migration in non-PAH and PAH HPASMC

Since non-PAH HPASMC showed only marginal non-stimulated migration, the pro-migratory factor PDGF was then used in both strains of cells (PAH and non-PAH). PDGF significantly promoted migration in both non-PAH and PAH strains of cells (Fig. 2). In the non-PAH cells PDGF activated migration by about three-fold. In the PAH HPASMC, PDGF significantly potentiated the already active dysregulated cell migration. A representative example is shown in fig. 2.

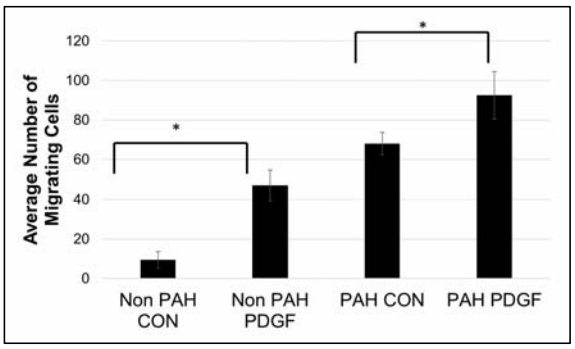

Fig. 2. Migration of HPASMC into wound after stimulation with or without 10 ng/ml PDGF. Bars represent the average of triplicate wells and error bars represent the standard deviation. *p < 0.05. Experiment was done using at least three non-PAH and three PAH strains with very similar results. Shown is a representative experiment using a non-PAH and PAH cell strain.

Involvement of the unstimulated PDGF receptor in PAH dysregulated migration

The involvement of PDGF and its receptor in promoting the migration of non-PAH and PAH cells into the wound area was determined using imatinib, an antibody against PDGF and a targeted PDGFR mimetic MMCPP (Tyr751P) [20]. Both imanitib and the PDGFR MMCPP significantly inhibited PDGF-stimulated migration of non-PAH cells. The antibody against PDGF also significantly inhibited this migration (Fig. 3A). As shown in fig. 3B, we tested the function of the unstimulated receptor to promote migration in PAH cells. The antibody was used to eliminate any possible effect by autologously produced PDGF. As shown in the figure the antibody had no significant effect. However, imatinib did inhibit migration as did the

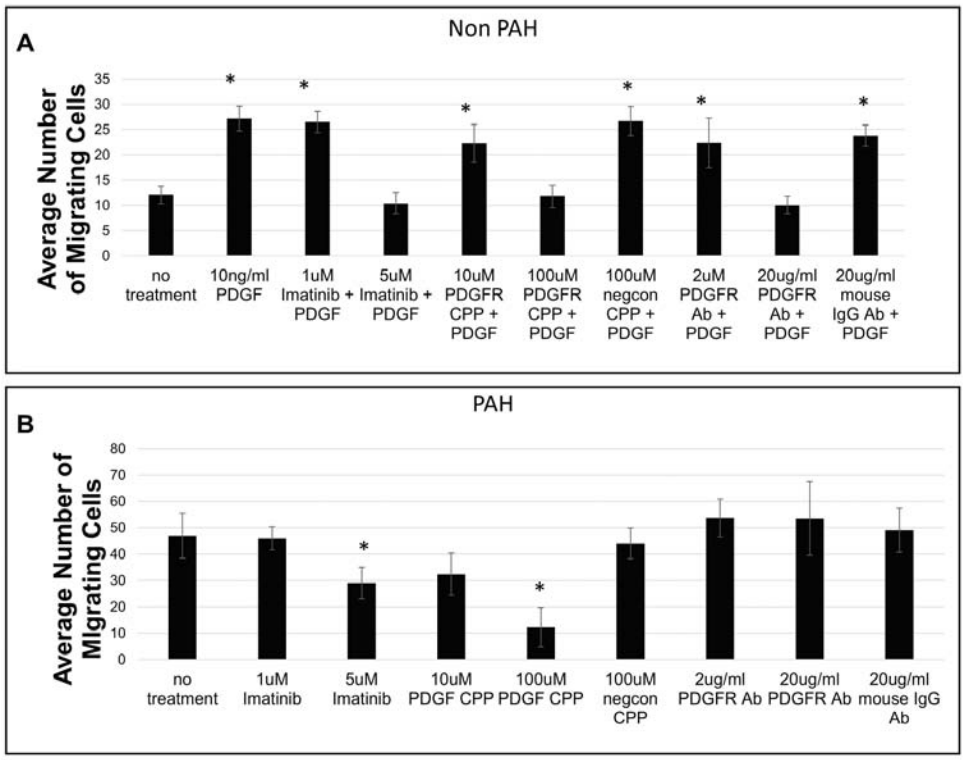

Fig. 3. PDGFR involved in PAH dysregulated migration. (A) Wound migration of non-PAH HPASMC treated with or without the PDGFR pharmacological inhibitor imatinib, PDGFR CPP (MMCPP mimicking the Try751P region of PDGFR) or neutralizing antibody (Ab) against PDGF ligands for 1 h before addition of 10 ng/ml PDGF. This experiment was repeated in three different non-PAH strains with (A) being representative of one. Bars represent the average number of migrating cells from triplicate wells. The standard deviation is represented by the error bars. (B) Wound migration of PAH HPASMC treated with or without imatinib, PDGFR MMCPP or neutralizing antibody (Ab) against PDGF. These experiments were repeated in three different PAH strains with (B) being representative of one. Negcon = negative control. *p < 0.05 vs no treatment.

PDGFR MMCPP. A negative control (negcon) MMCPP had no effect.

FAK and its expression in PAH HPASMC migration

FAK is known to be involved in cell adhesion and motility [13, 14]. FAK Tyr-397 phosphorylation has been described to lead to interaction with Src and consequent cell migration [27]. In fig. 4A we illustrate that total FAK expression is increased markedly in PAH cells in comparison to non-PAH. Consequently, FAK phosphorylated at the Tyr-397 position was detectable in the PAH cells but under equivalent conditions it was not detectable in the non-PAH cells. FAK kinase inhibitor PF-573228 eliminated the detection of phosphorylated Tyr-397 in PAH cells. Imanitib reduced the phosphorylation of FAK Tyr-397 by approximately 30%. As illustrated in fig. 4B, in non-PAH cells PDGF stimulation increased migration by approximately 2.5 fold. 5 uM FAK inhibitor brought it down to the level of basal migration. In PAH cells 5 uM FAK inhibitor plus imatinib reduced migration to the level of basal non-PAH cells. In the absence of imatinib it took 10 uM FAK inhibitor to bring migration down to the level of the non-PAH cells.

Effect of mitogen-activated protein (MAP) kinases on basal migration in PAH HPASMC

MAP kinases have been shown to be involved in cell migration [28]. MAP kinase inhibitors of JNK and p38 activation reduced migration in PAH HPASMC and PDGF-induced migration in non-PAH HPASMC (Fig. 5A-B).

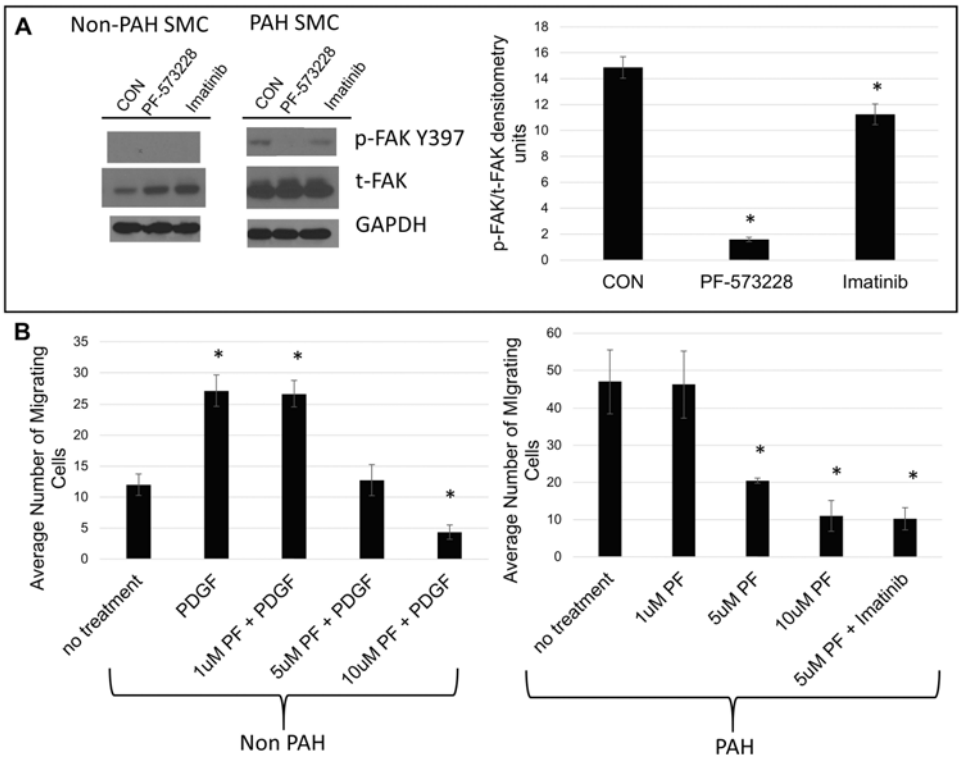

Fig. 4. Effect of FAK inhibitor on PAH HPASMC migration. (A) Western blot on HPASMC treated with or without 10 uM PF-573228 (PF) (FAK inhibitor) or 5 uM imatinib. Blots were probed for phosphorylated FAK (p-FAK) Y397, total FAK (t-FAK) and glyceraldehyde-3-phosphate dehydrogenase (GAPDH). Bar graphs represent the average densitometric units of p-FAK/t-FAK in triplicate experiments from PAH HPASMC and the error bars represent the standard deviation. *$p < 0.05$ vs control. (B) Bar graphs represent the average number of cells migrating into the wound area after treatment with or without various dosages of PF or imatinib (5 uM). The error bars represent the standard deviation. *$p < 0.05$ vs no treatment. These experiments were repeated in three different non-PAH and PAH strains. These graphs are representative of typical non-PAH and PAH HPASMC.

To confirm the activation of certain kinases at points of migration, immunofluorescence was performed on PAH HPASMC 15 minutes after wounding. HPASMC were probed for p-ERK (Extracellular signal-regulated kinases), p-p38 and p-JNK and imaged to detect the activated kinases in cells located at the edge of the wound as well as outside the wound area. The results are shown in Fig. 5C-E. p-ERK was activated but was evenly distributed throughout the culture (Fig. 5C), while both activated p38 and JNK were found only in the cells on the edge of the wound (Fig. 5D, E). Inhibitors of FAK, Rac and CDC42 activation all significantly reduced both p-p38 and p-JNK formation in the PAH cells at the wound's edge following culture injury (Fig. 5F, G). Representative images of blockage of signaling in cells at the edge of the wound are illustrated in S1 and S2 Figs.

Role of downstream kinases in non stimulated migration of PAH HPASMC

Two important kinases LIMK and PAK have been implicated in cell motility and have been described as acting downstream of Rac [18, 29]. As illustrated, chemical inhibition of each kinase (LIMK and PAK) in the PAH cells resulted in a predominant reduction in migration (Fig. 6).

Disruption of dysregulated PAH migration using key targeted MMCPP

Targeted MMCPPs were then synthesized to determine if the dysregulated self-activated migration could be perturbed at downstream targets. To accomplish this, MMCPP were targeted to block the action of two key cell migration regulators cofilin and CaD. The cofilin MMCPP (COF) mimics the actin binding domain of active cofilin which is a downstream target of LIMK [30]. The negative control, the P-COF peptide, has a similar sequence except that it contains a phosphorylated site at Ser-3 and mimics inactive cofilin. While the COF MMCPP caused a significant reduction in migration, P-COF had no effect (Fig. 7). For CaD, peptides which target the MAPK phosphorylation site of CaD (CaD-MAPK) or the PAK-mediated phosphorylation site (CaD-PAK) were synthesized [17]. Both of these peptides mimicked their respective CaD sites except that an Ala was substituted for Ser (Ser497 and Ser527 for CaD MAPK, Ser452 and Ser482 for CaD-PAK). The negative control, P-CaD-MAPK peptide, has the same sequence as CaD-MAPK except that the two Ser were substituted with Asp. Both CaD-MAPK and CaD-PAK completely knocked out the ability of PAH HPASMC to migrate, while P-CaD-MAPK only decreased migration by one-third (Fig. 7).

Cell viability

The effect of pharmacological inhibitors and MMCPP used in the experiments on cell viability was determined with the use of MTT assay. All treated cultures retained over 90% cell viability relative to untreated (no inhibitor) cultures with the exception of those exposed to hydrogen peroxide which retained only ~50% viability. This is illustrated in fig. 8.

DISCUSSION

Proliferation and migration of smooth muscle cells within and out of the arterial media into the injured endothelium and then into the lumina of the vessel in patients with PAH is a primary contributor to the deleterious symptoms and outcome of the disease. In a former communication we showed that PAH HPASMC display dysregulated proliferation [9]. As with proliferation of all the PAH cell strains tested, all demonstrated active PAH HPASMC migration under quiescent growth and non-stimulatory conditions. Non-PAH HPASMC under the same conditions showed only marginal motility. As illustrated, with blocked proliferation by the addition of a cell growth arresting agent and under cell plating conditions where little growth occurred within the time span of the experiment, migration was taking place in the absence of cell division. This dysregulated HPASMC migration has also been reported in SMC isolated from hypoxic rat pulmonary arteries [31].

The primary goal of this communication has been to elucidate the mechanism(s) regulating PAH derived HPASMC migration. Another objective of this communication has been to control this migration with MMCPP at points in the regulatory signal cascade(s) projected to be least intrusive with regard to the processes involved in normal physiology of the cells. Microscopic observations

showed dysregulated migration taking place in PAH cells at the edge of the wound. However, even in the absence of injury (barrier removal procedure) the PAH cells exhibited dysregulated motility. Non-PAH cells required a growth factor, such as PDGF, for substantial migration to occur. PDGF also promoted migration in PAH cells beyond that seen under unstimulated conditions.

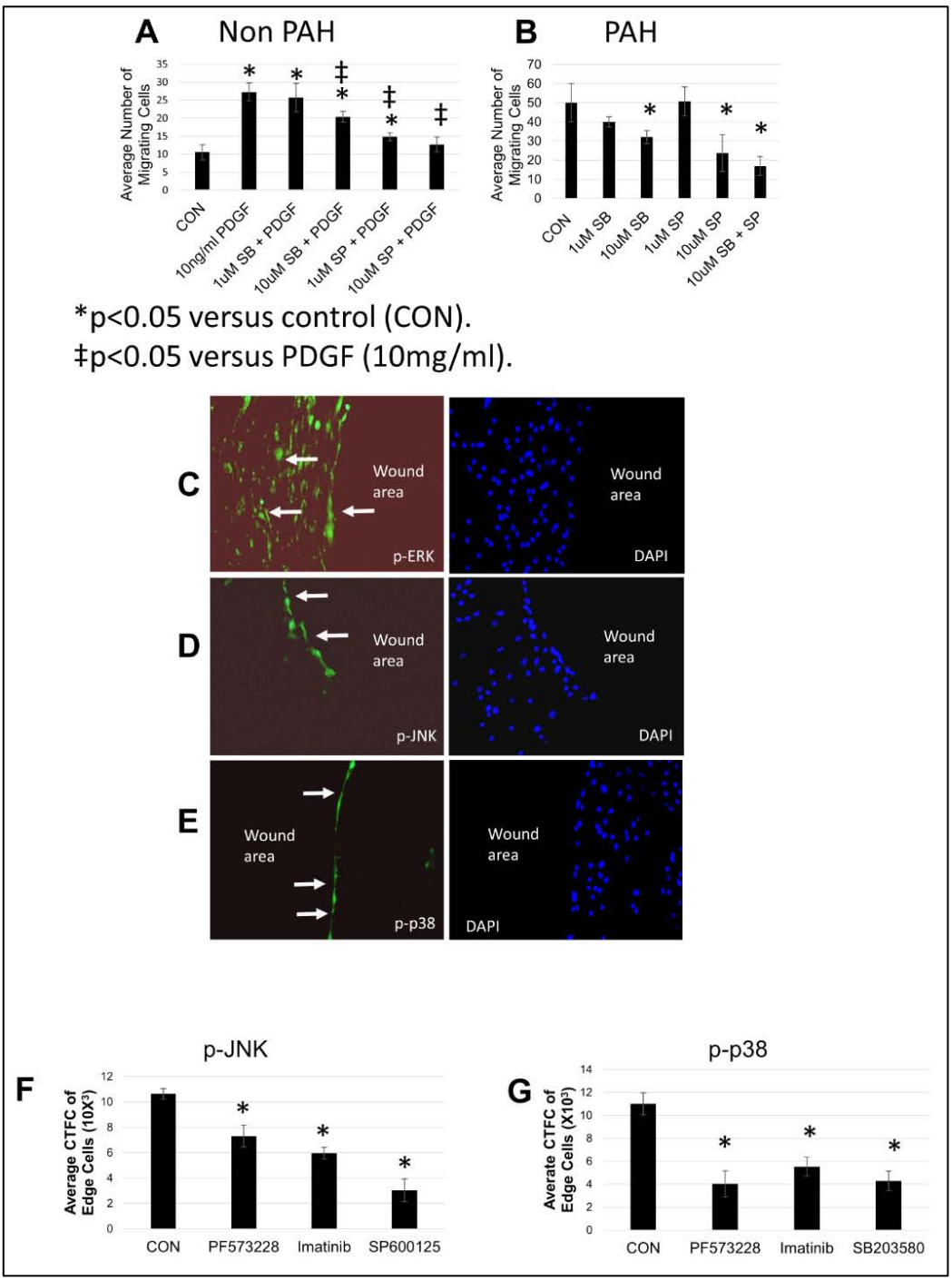

Fig. 5

The altered dysregulated migration of the PAH cells is not due to the PDGF released into the medium by the cells. As illustrated, elimination of any autologously produced PDGF with antibody did not alter the PAH cell motility. However, our results show that the dysregulated PAH migration is in part under control of the PDGFR. In the absence of PDGF stimulation, imatinib, a nonspecific tyrosine kinase inhibitor known to block PDGFR signaling, and a MMCPP directed against Tyr-751 phosphorylation site in the PDGFR effected a partial inhibition of the dysregulated migration. PDGF proved stimulatory to migration in both the PAH and non-PAH cells. However, migration experiments using anti-PDGF antibodies and imanitib illustrated that PDGFR itself, in the absence of activation by PDGF, is at least in part promoting the dysregulated migration in PAH cells.

The stimulation of migration by the PDGFR appears to be taking place through the activation of FAK as illustrated with imatinib inhibiting the phosphorylation of FAK at Tyr-397. Phosphorylation of FAK at Tyr-397 creates a high-affinity SH2 binding site for the Src-family [32] where the stimulated nucleation of signaling proteins bound to FAK can be initiated either through intrinsic autophosphorylation at Tyr-397 or through trans-phosphorylation of this site. Thus, Tyr-397 of FAK is the site which links with Src and in turn activates the cascade leading to actin reorganization and migration [33]. However, independent of the PDGFR, the expression of both phosphorylated Tyr-397 and unphosphorylated FAK is increased markedly in the PAH cells compared to non-PAH cells. This observation is confirmed by the results reported by Paulin *et al.*, 2014 [27] who also showed that in PAH cells FAK phosphorylation levels are increased.

Inhibition of FAK phosphorylation stops the dysregulated migration. Thus, our results strongly suggest that the increased expression of total and phosphorylated FAK and Src may be primary in the dysregulated migration of the PAH cells. As published by others, the FAK/Src complex has been shown to interact with small G-proteins [34-36]. Inhibiting the activation of the small G-proteins, Rac, CDC42 and RhoA have been reported to modulate cellular migration [16, 18, 37]. Our results confirm these regulatory points in the dysregulated HPASMC and PDGF-stimulated non-PAH cells. The only exception being that RhoA is not functioning in the dysregulated PAH cell migration. RhoA is known to be involved in stress fiber formation, but unlike Rac and CDC42, it is not directly involved in lamellipodia [38] or filopodia [39] formation which is key for cell migration. It appears that RhoA/ROCK is more central to HPASMC constriction [40] and retraction [41] rather than protrusion and translocation during cell migration. Likewise, limiting the activation of LIMK and PAK (further down the signaling pathway) regulates migration [18, 29]. Thus apparently the cascades leading to both the dysregulated motility and the PDGF-stimulated non-PAH motility in HPASMC follow similar routes through PDGFR and FAK cascades.

MAP kinases have been shown to participate in the migration of smooth muscle cells [28]. Here, we show with the use of inhibitors that both p38

Legend to Fig. 5. Effect of p38 and JNK inhibitors on HPASMC migration. A wound migration assay was performed on non-PAH (A) and PAH HPASMC (B) treated with or without p38 inhibitor SB203580 (SB) or JNK inhibitor SP600125 (SP). Bar graphs represent the average of triplicate wells with error bars representing the standard deviation. *$p < 0.05$ vs PDGF alone in non-PAH and *$p < 0.05$ vs control in PAH. These graphs are representative of a PAH HPASMC. Experiment was done using at least three PAH strains. Immunofluorescence on the wound's edge of PAH (C-E). Cells were fixed 15 minutes after wounding and probed for p-ERK (C), p-JNK (D) and p-p38 (E). Images are 200X magnification and arrows point to positively stained cells. The left column shows images probed with respective antibodies and the right column are the same images showing cells stained with DAPI. Experiments were also performed in the presence of inhibitors PF573228 (FAK inhibitor), SB203580 (p38 inhibitor) or SP600125 (JNK inhibitor) and also probed for p-JNK (F) and p-p38 (G) Corrected total cell fluorescence (CTCF) was calculated from at least seven cells on the wound edge per field. Average CTCF was computed from at least three fields of cells per slide and duplicate slides. Bars represent the average CTCF and the error bars represent the standard deviation. *$p < 0.05$ vs control.

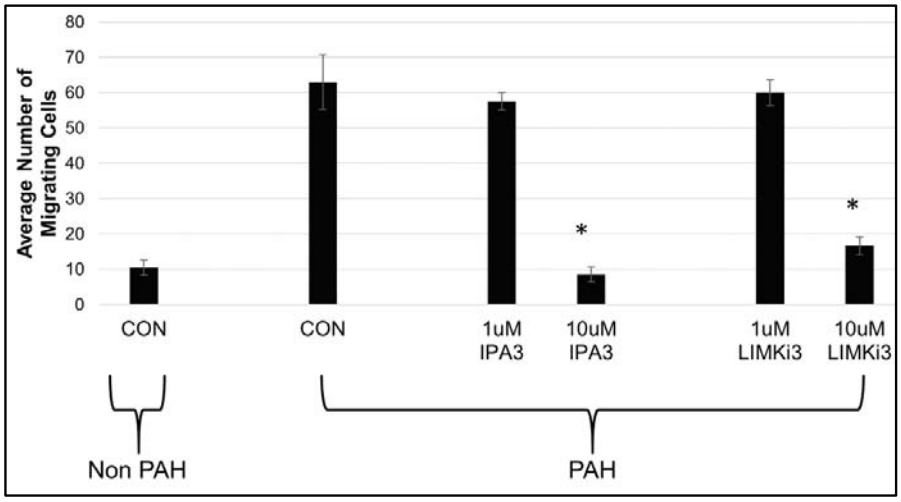

Fig. 6. Effect of LIMK and PAK inhibitors to regulate PAH HPASMC migration. A wound migration assay was performed on PAH HPASMC treated with or without IPA3 (PAK inhibitor) or LIMKi3 (LIM kinase inhibitor). Bar graphs represent the average of triplicate wells and the error bars represent the standard deviation. *p < 0.05 vs control in PAH. These graphs are representative of a typical PAH HPASMC. Experiment was done using at least three PAH strains. A typical non-PAH basal migration is represented in the graph for relative comparision.

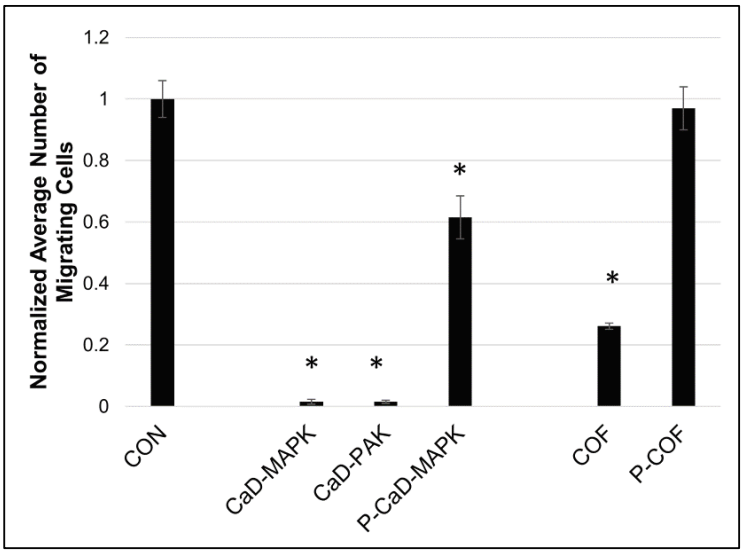

Fig. 7. Effect of MMCPPs targeting CaD and cofilin on PAH HPASMC migration. A wound migration assay was performed on PAH HPASMC treated with or without designated MMCPP (20 uM each). Bar graphs represent the normalized average number of triplicate experiments and the error bars represent the standard deviation. Normalized average was calculated by dividing all treatments by the average number of migrating untreated cells (CON). This was used in order to combine results from different experiments performed independently. These graphs are representative of a typical PAH HPASMC. Experiment was done using at least three PAH strains. *p < 0.05 vs CON. CaD-MAPK and CaD-PAK peptides target MAP kinase and PAK sites of CaD, respectively. P-CaD-MAPK is similar to CaD-MAPK except for a Ser substituted for Asp. COF peptide mimicks active cofilin while p-COF mimics inactive cofilin.

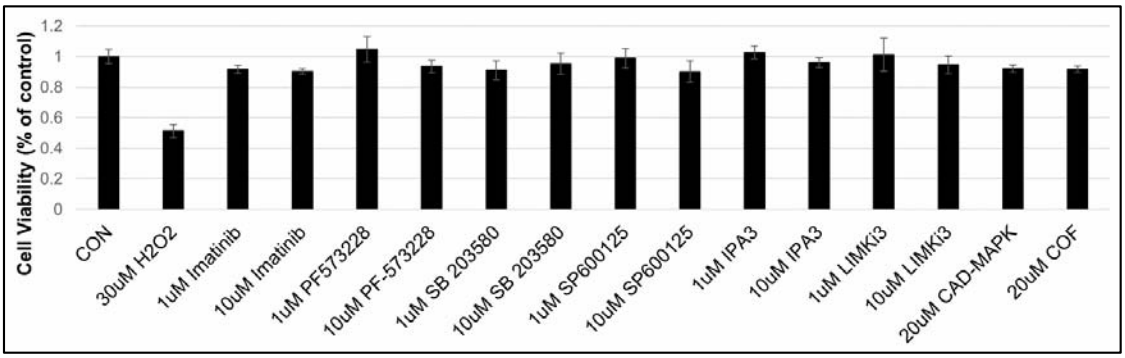

Fig. 8. MTT assay showing cell viablity after exposure to pharmacological inhibitors or MMCPP for 24 hours. HPASMC were treated with or without respective amounts of imatinib, FAK inhibitor (PF-573228), p38 inhibitor (SB 203580), JNK inhibitor (SP 600125), PAK inhibitor (IPA3), LIMK inhibitor (LIMKi3), CaD-MAPK MMCPP or COF MMCPP. MTT OD was measured and normalized to the average of untreated (CON) cells for determining percentage of cell viablity. Each treatment was done in triplicate and error bars represent the standard deviation. This graph is representative of independent experiments performed on three different PAH HPASMC.

and JNK are part of the cascade regulating PDGF-induced migration in non-PAH HPASMC and migration of unstimulated PAH HPASMC. Our results using immunofluorescence microscopy show that in PAH cells while ERK, p38 and JNK are all activated following culture injury, the activation of ERK is distributed throughout the culture. However, JNK and p38 are activated only at the edge of the injury.

In a previous communication we showed that the Tyr751P MMCPP was able to limit the PDGF-promoted wound migration of non-PAH HPASMC [20]. Here, we show that MMCPP which inhibit PAK as well as MAPK phosphorylation sites of CaD block cell migration. Also a MMCPP which mimics the actin binding site of cofilin [42] arrests the migration of PAH HPASMC.

Combining our own results with those published by others has led us to postulate the cascades shown in fig. 9 leading to HPASMC migration. We are projecting two fundamental end points promoting migration in PAH cells with FAK being central, then diverting downstream to CaD phosphorylation through PAK, JNK and p38 and cofilin phosphorylation/dephosphorylation through LIMK [15] and slingshot phosphatase [19] (Fig. 9). By shutting down either CaD phosphorylation or cofilin phosphorylation/dephosphorylation with MMCPP we were able to block the migration of the PAH cells.

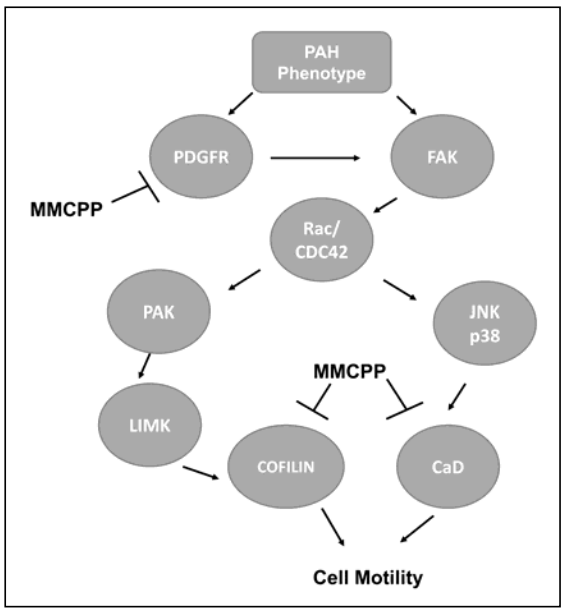

Fig. 9. Outline of proposed PAH HPASMC migration signal cascades. Arrows represent the relationships between these proteins in promoting cell migration in PAH HPASMC.

As stated, the primary goal of this communication has been to understand the mechanism(s) operating in the dysregulated migration in PAH HPASMC and then begin to control this dysregulated migration at point(s) considered least physiologically intrusive. For example, while FAK is an available target, it is far upstream. It has been shown to be

physiologically important in insulin signaling [43] and to be cardio protective [44-46]. Thus modulating the functions of downstream targets such as cofilin or CaD with MMCPP could be very advantageous.

CONCLUSION

In conclusion, we find that targeted MMCPP can be utilized to regulate both the PDGF-promoted and the dysregulated PAH HPASMC migration. Results further suggest that a malfunctioning PDGF receptor is participating in promoting the dysregulated migration. The hyper-migratory nature of PAH HPASMC very likely contributes to vascular remodeling taking place in PAH and finely targeted MMCPP can potentially ameliorate the pathology of this fatal disease.

ACKNOWLEDGEMENTS

We thank The Cleveland Clinic Pathobiology Tissue Sample and Cell Culture Core (supported by NIH PO1 HL081064 and RC37 HL60917) and Dr. Marlene Rabinovitch, Stanford University under the Pulmonary Hypertension Breakthrough Initiative (PHBI) supported by the Cardiovascular Medical Research and Education Fund for pulmonary smooth muscle cell samples. This study was supported in part by National Institutes of Health/National Lung, Heart, and Blood Institute Grant HL25776.

CONFLICT OF INTEREST STATEMENT

The authors have no conflicts of interest relating to this manuscript.

SUPPLEMENTARY FIGURES

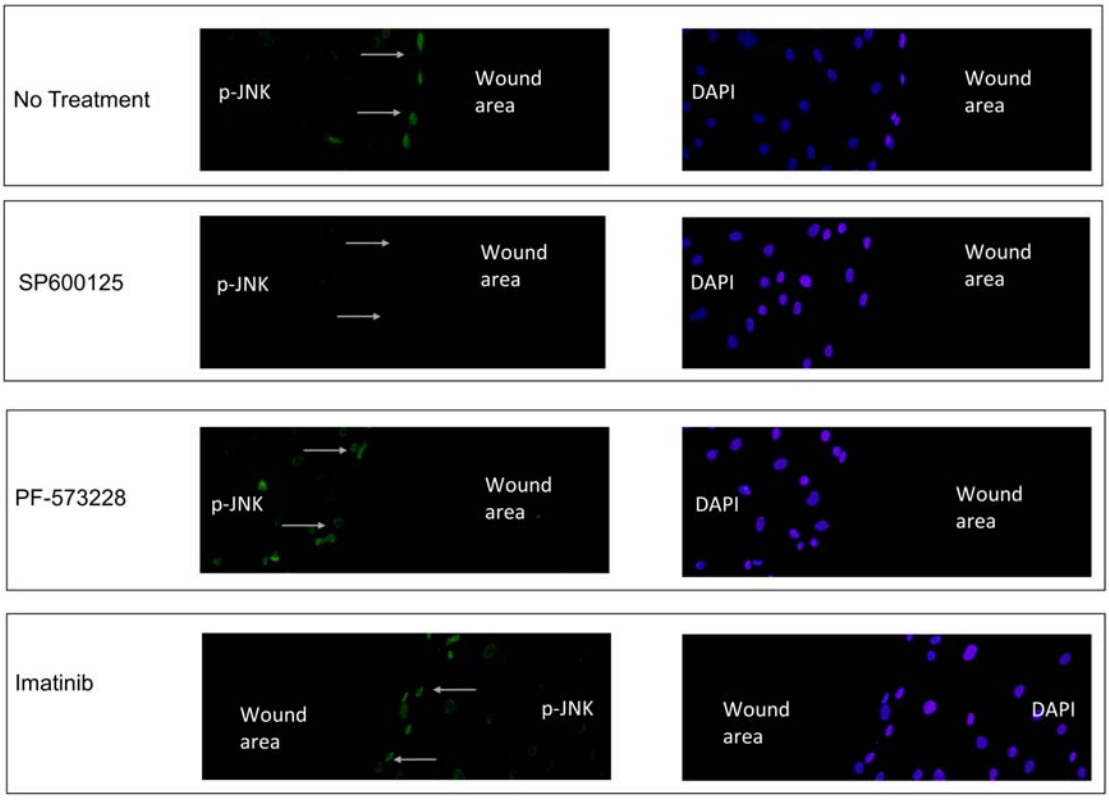

Fig. S1. Immunofluorescence microscopy images of PAH HPASMC probed for p-JNK after inhibition. Images are 200X magnification and arrows point to positively stained cells. The left column shows images probed with respective antibodies and the right column are the same images showing cells stained with DAPI. Experiments were also performed in the presence of inhibitors SP600125 (JNK inhibitor), PF573228 (FAK inhibitor) or imatinib and probed for p-JNK.

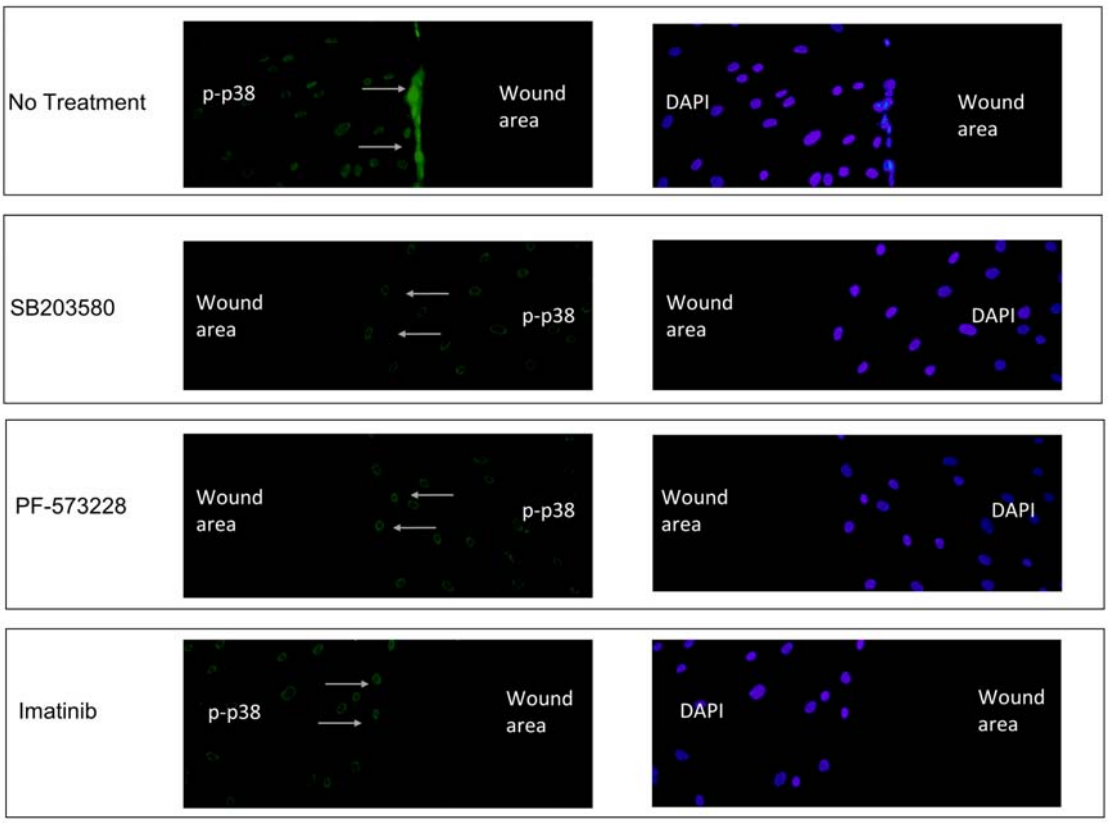

Fig. S2. Immunofluorescence microscopy images of PAH HPASMC probed for p-p38 after inhibition. Images are 200X magnification and arrows point to positively stained cells. The left column shows images probed with respective antibodies and the right column are the same images showing cells stained with DAPI. Experiments were also performed in the presence of inhibitors SB203580 (p38 inhibitor), PF573228 (FAK inhibitor) or imatinib and probed for p-p38.

REFERENCES

1. Schwartz, S. M. 1997, J. Clin. Invest., 100(11 Suppl.), S87.
2. Tajsic, T. and Morrell, N. W. 2011, Compr. Physiol., 1, 295.
3. Perros, F., Dorfmuller, P., Souza, R., Durand-Gasselin, I., Godot, V., Capel, F., Adnot, S., Eddahibi, S., Mazmanian, M., Fadel, E., Hervé, P., Simonneau, G., Emilie, D. and Humbert, M. 2007, Eur. Respir. J., 29, 937.
4. Rydell-Tormanen, K., Risse, P. A., Kanabar, V., Bagchi, R., Czubryt, M. P. and Johnson, J. R. 2013, Pulm. Pharmacol. Ther., 26, 13.
5. Frazier, A. A. and Burke, A. P. 2012, Semin. Ultrasound. CT. MR., 33, 535.
6. Jonigk, D., Golpon, H., Bockmeyer, C. L., Maegel, L., Hoeper, M. M., Gottlieb, J., Nickel, N., Hussein, K., Maus, U., Lehmann, U., Janciauskiene, S., Welte, T., Haverich, A., Rische, J., Kreipe, H. and Laenger, F. 2011, Am. J. Pathol., 179, 167.
7. Sheikh, A. Q., Lighthouse, J. K. and Greif, D. M. 2014, Cell Rep., 6, 809.
8. Goncharov, D. A., Kudryashova, T. V., Ziai, H., Ihida-Stansbury, K., DeLisser, H., Krymskaya, V. P., Tuder, R. M., Kawut, S. M. and Goncharova, E. A. 2014, Circulation, 129, 864.
9. Wilson, J. L., Yu, J., Taylor, L. and Polgar, P. 2015, PLoS One, 10, e0123662.
10. Zhang, S., Fantozzi, I., Tigno, D. D., Yi, E. S., Platoshyn, O., Thistlethwaite, P. A., Kriett, J. M., Yung, G., Rubin, L. J. and Yuan, J. X. 2003, Am. J. Physiol. Lung Cell. Mol. Physiol., 285, L740.

11. Perros, F., Montani, D., Dorfmuller, P., Durand-Gasselin, I., Tcherakian, C., Le Pavec, J., Mazmanian, M., Fadel, E., Mussot, S., Mercier, O., Hervé, P., Emilie, D., Eddahibi, S., Simonneau, G., Souza, R. and Humbert, M. 2008, Am. J. Respir. Crit. Care. Med., 178, 81.
12. Capdeville, R., Buchdunger, E., Zimmermann, J. and Matter, A. 2002, Nat. Rev. Drug. Discov., 1, 493.
13. Louis, S. F. and Zahradka, P. 2010, Exp. Clin. Cardiol., 15, e75-85.
14. Sieg, D. J., Hauck, C. R., Ilic, D., Klingbeil, C. K., Schaefer, E., Damsky, C. H. and Schlaepfer, D. D. 2000, Nat. Cell Biol., 2, 249.
15. Dai, Y. P., Bongalon, S., Tian, H., Parks, S. D., Mutafova-Yambolieva, V. N. and Yamboliev, I. A. 2006, Vascul. Pharmacol., 44, 275.
16. Huang, M., Satchell, L., Duhadaway, J. B., Prendergast, G. C. and Laury-Kleintop, L. D. 2011, J. Cell. Biochem., 112, 1572.
17. Jiang, Q., Huang, R., Cai, S. and Wang, C. L. 2010, J. Biomed. Sci., 17, 6.
18. Moshfegh, Y., Bravo-Cordero, J. J., Miskolci, V., Condeelis, J. and Hodgson, L. 2014, Nat. Cell Biol., 16, 574.
19. San Martin, A., Lee, M. Y., Williams, H. C., Mizuno, K., Lassegue, B. and Griendling, K. K. 2008, Circ. Res., 102, 432.
20. Yu, J., Rupasinghe, C., Wilson, J. L., Taylor, L., Rahimi, N., Mierke, D. and Polgar, P. 2015, Chem. Biol. Drug Des., 85, 586.
21. Drin, G., Cottin, S., Blanc, E., Rees, A. R. and Temsamani, J. 2003, J. Biol. Chem., 278, 31192.
22. Green, D. S., Rupasinghe, C., Warburton, R., Wilson, J. L., Sallum, C. O., Taylor, L., Yatawara, A., Mierke, D., Polgar, P. and Hill, N. 2013, PLoS One. 8, e81309.
23. Aldred, M. A., Comhair, S. A., Varella-Garcia, M., Asosingh, K., Xu, W., Noon, G. P., Thistlethwaite, P. A., Tuder, R. M., Erzurum, S. C., Geraci, M. W. and Coldren, C. D. 2010, Am. J. Respir. Crit. Care Med., 182, 1153.
24. Comhair, S. A., Xu, W., Mavrakis, L., Aldred, M. A., Asosingh, K. and Erzurum, S. C. 2012, Am. J. Respir. Cell Mol. Biol., 46, 723.
25. Schneider, C. A., Rasband, W. S. and Eliceiri, K. W. 2012, Nat. Methods, 9, 671.
26. Burgess, A., Vigneron, S., Brioudes, E., Labbe, J. C., Lorca, T. and Castro, A. 2010, Proc. Natl. Acad. Sci. USA, 107, 12564.
27. Paulin, R., Meloche, J., Courboulin, A., Lambert, C., Haromy, A., Courchesne, A., Bonnet, P., Provencher, S., Michelakis, E. D. and Bonnet, S. 2014, Eur. Respir. J., 43, 531.
28. Kavurma, M. M. and Khachigian, L. M. 2003, J. Cell. Biochem., 89, 289.
29. Edwards, D. C., Sanders, L. C., Bokoch, G. M. and Gill, G. N. 1999, Nat. Cell Biol., 1, 253.
30. Eibert, S. M., Lee, K. H., Pipkorn, R., Sester, U., Wabnitz, G. H., Giese, T., Meuer, S. C. and Samstag, Y. 2004, Proc. Natl. Acad. Sci. USA, 101, 1957.
31. Meoli, D. F. and White, R. J. 2010, Can. J. Physiol. Pharmacol., 88, 830.
32. Schlaepfer, D. D. and Mitra, S. K. 2004, Curr. Opin. Genet. Dev., 14, 92.
33. Schlaepfer, D. D., Hauck, C. R. and Sieg, D. J. 1999, Prog. Biophys. Mol. Biol., 71, 435.
34. Lim, Y., Lim, S. T., Tomar, A., Gardel, M., Bernard-Trifilo, J. A., Chen, X. L., Uryu, S. A., Canete-Soler, R., Zhai, J., Lin, H., Schlaepfer, W. W., Nalbant, P., Bokoch, G., Ilic, D., Waterman-Storer, C. and Schlaepfer, D. D. 2008, J. Cell Biol., 180, 187.
35. Ren, X. D., Kiosses, W. B., Sieg, D. J., Otey, C. A., Schlaepfer, D. D. and Schwartz, M. A. 2000, J. Cell Sci., 113, 3673.
36. Tomar, A., Lim, S. T., Lim, Y. and Schlaepfer, D. D. 2009, J. Cell Sci., 122, 1852.
37. Cui, Y., Sun, Y. W., Lin, H. S., Su, W. M., Fang, Y., Zhao, Y., Wei, X. Q., Qin, Y. H., Kohama, K. and Gao, Y. 2014, Mol. Cell. Biochem., 393, 255.
38. Ballestrem, C., Wehrle-Haller, B., Hinz, B. and Imhof, B. A. 2000, Mol. Biol. Cell, 11, 2999.
39. Krugmann, S., Jordens, I., Gevaert, K., Driessens, M., Vandekerckhove, J. and Hall, A. 2001, Curr. Biol., 11, 1645.

40. Ridley, A. J. and Hall, A. 1992, Cell, 70, 389.
41. Smith, A., Bracke, M., Leitinger, B., Porter, J. C. and Hogg, N. 2003, J. Cell Sci., 116, 3123.
42. Arber, S., Barbayannis, F. A., Hanser, H., Schneider, C., Stanyon, C. A., Bernard, O. and Caroni, P. 1998, Nature, 393, 805.
43. Cai, E. P., Casimir, M., Schroer, S. A., Luk, C. T., Shi, S. Y., Choi, D., Dai, X. Q., Hajmrle, C., Spigelman, A. F., Zhu, D., Gaisano, H. Y., MacDonald, P. E. and Woo, M. 2012, Diabetes, 61, 1708.
44. Hakim, Z. S., DiMichele, L. A., Rojas, M., Meredith, D., Mack, C. P. and Taylor, J. M. 2009, J. Mol. Cell. Cardiol., 46, 241.
45. Perricone, A. J., Bivona, B. J., Jackson, F. R. and Vander Heide, R. S. 2013, J. Am. Heart Assoc., 2, e000457.
46. Vander Heide, R. 2011, J. Cardiovasc. Pharmacol. Ther., 16, 251.